THE JOURNAL OF COMPARATIVE NEUROLOGY 305:35–48 (1991)

Synaptic Connections of the Auditory Nerve in Cats: Relationship Between Endbulbs of Held and Spherical Bushy Cells

DAVID K. RYUGO AND SEISHIRO SENTO
Department of Otolaryngology-Head and Neck Surgery, Center for Hearing Sciences, Johns Hopkins University School of Medicine, Baltimore, Maryland 21205 (D.K.R.), and Department of Medical Science Research, Yuai Clinic, Saitama 331, Japan (S.S.)

ABSTRACT

This report focuses on a class of large synaptic endings, the endbulbs of Held. These endings are located in the anteroventral cochlear nucleus and arise from the axons of type I spiral ganglion neurons. Axons were stained with horseradish peroxidase (HRP) using intracellular injections of single fibers or extracellular injections into the auditory nerve. Individual endbulbs or pairs of endbulbs that converged onto the same spherical bushy cell were examined with the aid of a light microscope and subjected to morphometric analyses. Endbulbs of fibers having low spontaneous discharge rates (SR, ≤ 18 spikes/sec) have a more complex shape than those of high SR fibers (> 18 s/s), a feature represented by systematic differences in endbulb silhouette perimeter without differences in endbulb silhouette area. Consequently, the ratio, silhouette area divided by silhouette perimeter, yields a "form factor" separating endbulbs of high SR from those of low SR. High SR fibers had ratios > 0.52 (mean $= 0.63 \pm 0.09$), whereas low SR fibers had ratios < 0.52 (mean $= 0.45 \pm 0.06$). Pairs of endbulbs with unknown physiological properties had similar form factor values, despite the wide range of values observed in the endbulb population. These data imply that endbulbs converging upon the cell body of a spherical bushy cell arise from fibers of the same SR group.

Electron microscopic examination was conducted on the endbulb of one physiologically characterized and intracellularly stained auditory nerve fiber (CF = 1.4 kHz; SR = 55 s/s) and its unstained endbulb mate with the aid of serial ultrathin sections. In addition to the well-known axosomatic synapses, these endbulbs formed axodendritic synapses: 11.7% for the HRP-labeled endbulb and 13.3% for the unlabeled endbulb. The axodendritic synapses appear to occur on dendrites of nearby spherical bushy cells and may represent a mechanism whereby single endbulbs can disperse activity to multiple neurons in the cochlear nucleus. We propose that axosomatic synapses preserve fiber SR groupings, whereas axodendritic synapses may not.

Key words: cochlear nucleus, electron microscopy, hearing, horseradish peroxidase, primary afferents, spontaneous activity

The obligatory synaptic termination of auditory nerve fibers in the cochlear nucleus provides the first site for recoding of neural information arising in the cochlea. The auditory code (that is, the pattern of spike discharges) entering the nucleus is qualitatively similar across all fibers for a broad range of stimulus conditions (Kiang et al., '65). In the cochlear nucleus, however, this code can be preserved or transformed (Pfeiffer, '66). The resulting output signals are then sent to higher auditory centers along pathways hypothesized to convey different features of this information (Warr, '82). One pathway that is of interest to us tightly couples neural activity to acoustic events such that timing information for the localization of a sound source is faithfully maintained (Konishi, '86).

In the anteroventral cochlear nucleus (AVCN), large endings of type I auditory nerve fibers, called endbulbs of Held, make axosomatic synapses with spherical bushy cells (Lenn and Reese, '66; Ibata and Pappas, '76; Cant and Morest, '79b; Ryugo and Fekete, '82). The regional overlap

Accepted November 1, 1990.

Address reprint requests to Dr. D.K. Ryugo, Traylor Research Building, Room 510, Center for Hearing Sciences, Johns Hopkins University School of Medicine, Baltimore, MD 21205.

between endbulbs, anatomically defined spherical bushy cells, and physiologically defined primarylike units with prepotentials has led to the suggestion that endbulbs transfer discharges of individual auditory nerve fibers in a 1-to-1 fashion to spherical bushy cells, thus producing the primarylike discharge patterns observed in the nucleus (Pfeiffer, '66; Bourk, '76; Tsuchitani, '78; Cant and Morest, '84). If spherical bushy cells act as simple relays, then the population of primarylike units with prepotentials should reflect the physiological features of the population of auditory nerve fibers by which they are innervated. In the auditory nerve, approximately 30–40% of the fibers have spontaneous discharge rates (SR) below 20 s/s (Kiang et al., '65; Liberman, '78). In the AVCN, however, the proportion of primarylike units with prepotentials and SR <20 s/s is less than 15% (Molnar and Pfeiffer, '68; Bourk, '76; T. Yin, personal communication). Because spontaneous activity in the ventral cochlear nucleus is derived from the auditory nerve (Koerber et al., '66), the question arises as to how the primary activity from endbulbs is transferred to spherical bushy cells to produce the observed alteration of SR distribution in the nucleus.

In the present study, we used light and electron microscopic examination of endbulbs labeled with horseradish peroxidase (HRP) to explore various structural mechanisms that might help to explain the electrophysiological data. We produced light microscopic evidence suggesting that endbulbs of the same SR group converge together onto the cell body of the same spherical bushy cell and that endbulbs of different SR groups do not. Electron microscopic evidence revealed that endbulbs can synapse onto the dendrites of nearby cells, thereby providing a mechanism for individual endbulbs to disperse neural activity to multiple neurons in the AVCN.

METHODS

Animal preparation and histological procedures

Healthy adult cats were used for the HRP labeling of auditory nerve fibers. Animals were anesthetized with intraperitoneal injections (0.2 cc per kg body weight) of diallyl barbituric acid (100 mg/ml) in urethane solution (400 mg/ml). Supplemental doses of Dial were administered when necessary to keep the animal areflexic. Body temperature was monitored with a rectal thermometer and maintained at 37°C using a circulating warm water pad.

After cannulation of the trachea, the animal was placed in a headholder, the posterior fossa was surgically opened using a dorsal approach, and the cerebellum was retracted toward the midline to expose the auditory nerve. In 6 cats, extracellular injections were made into the nerve using a glass micropipette filled with a solution of HRP (Sigma type VI, 20–30% w/v in 0.1 M Tris buffer, pH 7.6). Pipettes were inserted into the nerve under direct visual control and HRP was ejected electrophoretically (2 microamps, positive current, 50% duty cycle) through the pipette tip (20–50 μm, I.D.). In 32 cats, intracellular injections were made. For each unit, a tuning curve and a 15- or 30-second sample of spontaneous activity were obtained before and after the injection of HRP. Fibers were labeled by iontophoresing a 10% solution of HRP (Sigma type VI) in 0.05 M Tris buffer (pH 7.3) containing 0.15 M KCl through micropipettes bevelled to a final impedance of 40–60 MΩ.

After approximately 24 hours, each animal was administered a lethal dose of Nembutal and perfused through the heart with 50 cc of isotonic saline (37°C) with 0.1% $NaNO_2$ followed by 1 L of fixative containing 0.5% paraformaldehyde and 1.0% glutaraldehyde in a 0.12 M phosphate buffer with 0.008% $CaCl_2$, and then a second liter of fixative containing 1.25% paraformaldehyde, 2.5% glutaraldehyde, and 0.008% $CaCl_2$ in the same phosphate buffer. The brainstem was partially exposed and immersed in cold fixative (6–18 hours, 5°C). The brain was then dissected from the skull and the cochlear nucleus sectioned on a Vibratome into 60-μm-thick sections and kept in serial order. The sections were rinsed several times in 0.1 M Tris buffer (pH 7.6) and then incubated for 1 hour in a solution of 0.5% $CoCl_2$ in Tris buffer. These sections were next washed in Tris buffer, washed in 0.1 M phosphate buffer (pH 7.3), and then incubated for 1 hour in a solution of 0.05% 3,3′-diaminobenzidine (Sigma), 0.01% H_2O_2, and 1% dimethylsulfoxide in phosphate buffer (pH 7.3). Sections were washed again and then mounted on glass microscope slides and counterstained with cresyl violet. Otherwise, sections were postfixed with 0.1% OsO_4 for 15 minutes, stained en bloc with 1% uranyl acetate (overnight), dehydrated, infiltrated with Epon, and flat-embedded between 2 sheets of Aclar (Allied Engineering Plastics, Pottsdam, PA). Tissue was studied using a light microscope. One HRP-labeled endbulb was isolated in a separate tissue block, thin sectioned, and examined with an electron microscope.

Golgi-impregnated brains from adult cats were also available for examination in studying the relationship between dendrites and cell bodies of spherical bushy cells. This material was prepared using the Golgi Cox (Van der Loos, '56) or Golgi Kopsch methods (Colonnier, '64; Adams, '79), embedded in Parlodion, and cut into 100-μm-thick sections.

Data analysis

We have combined Liberman's ('78) low (<0.5 s/s) and medium (0.5–18 s/s) SR groups into a single low SR group (SR $\leq$ 18 s/s) because we have not found any anatomical distinctions between his low and medium SR categories (Fekete et al., '84; Rouiller et al., '86; Ryugo and Rouiller, '88; Sento and Ryugo, '89). High SR fibers have discharge rates >18 s/s. The ratio of endbulb silhouette area divided by endbulb silhouette perimeter (units dropped) yields a "form factor" that is a reliable indicator of fiber SR (Sento and Ryugo, '89). Of 46 endbulbs, there was one exception from each SR group. In general, a form factor value >0.52 (mean $= 0.63 \pm 0.09$) is characteristic of an endbulb from a high SR fiber, whereas a value <0.52 (mean $= 0.45 \pm 0.06$) is typical of an endbulb from a low SR fiber. We applied this light microscopic algorithm to pairs of converging endbulbs that were labeled by extracellular injections of HRP into the auditory nerve.

Endbulb pairs, darkly stained and located well within the tissue section, were selected for analysis. Each endbulb of the pair was drawn with the aid of a light microscope and drawing tube at a total magnification of 1875×. Pairs were chosen for study when a reconstruction demonstrated that each endbulb arose from separate fibers. Overlapping parts of these complex, three-dimensional structures were optically separated with the light microscope by using different focal planes while drawing. The somatic outline of the postsynaptic spherical bushy cell was drawn at its largest diameter. All drawings were photographically enlarged to a final magnification of 3750×, and then silhouette areas and

perimeters were determined by computerized planimetry (SigmaScan, Jandel Scientific). Means, standard deviations, correlation coefficients (r), t-test values, and p values are provided when appropriate.

Electron microscopy

We analyzed several endbulbs of Held with the aid of an electron microscope. One HRP-labeled endbulb and one unlabeled endbulb that contacted the same spherical bushy cell were studied using serial ultrathin sections. In addition, several nearby unlabeled endbulbs were also examined. Typically, 6–8 electron micrographs were required to circumscribe the somatic perimeter of the spherical bushy cell and its presynaptic endings. Photomontages were made at a total magnification of 14,100×. Each montage was then photographically copied onto a 4″ × 5″ negative and reprinted at a total magnification of 10,000×. These smaller montages were more convenient in size and structures of interest (e.g., labeled endbulb, unlabeled primary terminals, nonprimary terminals, dendritic profiles, spherical cell body, postsynaptic densities) could still be unambiguously identified by using the montages at both magnifications.

RESULTS

Intracellular injections of HRP have been shown to label the entire axonal arborization of individual auditory nerve fibers, including en passant and terminal endings (Fekete et al., '84; Rouiller et al., '86; Ryugo and Rouiller, '88). Endbulbs of Held are one class of auditory nerve endings that are operationally defined as large axosomatic terminations, composed of 14 or more components (lobules, swellings, and branches), and located in the AVCN at the tip of the ascending branch of type I auditory nerve fibers (Rouiller et al., '86). Within a few micrometers of the target cell body, each fiber loses its myelin sheath and arborizes over the somatic surface to form the endbulb. The unmyelinated trunk divides into several knobby branches from which thinner branches arise. The branches ramify further and form a network of lobes and varicosities interconnected by fine processes. These complex, claw-shape arborizations cradle the postsynaptic cell body. All terminal endbulbs in this report are localized within the anterior division of the anteroventral cochlear nucleus (see Fig. 2 of Fekete et al., '84).

The appearance of endbulbs from fibers of the separate SR groupings is distinctive for each group and is illustrated in Figure 1. This difference can be quantified by the form factor (Sento and Ryugo, '89). Form factor value is correlated with fiber SR ($r = 0.634$, $p < 0.01$), and endbulbs of the high SR group (≥ 18 s/s) typically have a ratio greater than 0.52. The larger form factor of high SR fibers results from a relatively smaller perimeter, apparently created by the fewer but larger varicosities and associated terminal swellings (Fig. 2). The appearance of the endbulb from the low SR fiber is also typical for its SR grouping in that it exhibits a delicate network of many small varicosities and associated terminal swellings. For this reason, endbulbs of the low SR group (≤ 18 s/s) have relatively larger perimeters and almost always have a ratio less than 0.52. We reasoned that pairs of endbulbs that converged onto the same cell body could be assigned to an SR group using this form factor analysis.

Endbulb pairs

Extracellular injections of HRP into the auditory nerve label auditory nerve fibers, the number of which (tens to thousands) depends upon the extent of damage to nerve fibers and the amount of HRP deposited. Most of these fibers are 2–4 μm in diameter and are clearly identifiable as the central axons of type I spiral ganglion neurons (Ryugo and Fekete, '82; Fekete et al., '84; Liberman and Oliver, '84). Although the combined number of labeled type I auditory nerve fibers across animals was quite large (several thousand), we found fewer than 100 instances where two endbulbs converged upon the same cell in the anterior division of the AVCN, and no instance where three endbulbs converged. Nineteen darkly stained and unambiguous endbulb pairs have been analyzed, where separate fibers give rise to converging endbulbs and where both endbulbs appear to be contained entirely within the same tissue section.

The structural relationship of two fibers forming an endbulb pair is strikingly complex (Fig. 3). Large caliber fibers (2–4 μm in diameter) approach the target bushy cell from different directions, often by abruptly reversing directions from their original trajectory. Auditory nerve fibers whose endbulbs ultimately converge onto the same cell body do not necessarily travel side-by-side; ascending branches can be separated by more than 100 μm. The envelope fashioned by the terminal swellings of each endbulb arbor establishes an irregular domain, and there appears to be a complementary interdigitation between domains of the separate endbulbs. Compared to the distinct appearance of endbulbs from fibers of different SR groups, the endbulbs belonging to a pair have remarkably similar appearances.

Endbulb silhouette area (size) for the 19 pairs ranged from 69.6–726.5 μm^2. For descriptive purposes, we call the smaller endbulb of the pair "endbulb 1" and the larger "endbulb 2." Although pairs of terminal endbulbs contacting the same spherical bushy cell are usually different in size, pairs are not formed by the largest and the smallest endbulbs in the population. This observation is based on the size distribution of endbulb pairs within a larger endbulb sample (Fig. 4). Instead, pairs of endbulbs tend to be correlated in area ($r = 0.864$, $p < 0.001$). Overall, the larger the cell body, the larger the endbulbs it tends to receive ($n = 69$, $r = 0.584$, $p < 0.01$).

Form factors for individual endbulbs of a pair ranged from 0.27–0.83. If endbulbs of fibers from the separate SR groups converged more-or-less randomly onto the same cell body, the ratio, form factor 1 (from endbulb 1) divided by form factor 2 (from endbulb 2), could produce a range of values from 0.32–3.07. In contrast, if endbulbs of fibers from the same SR groups converged, this ratio should have a range of values near 1.0. In fact, the average ratio is 0.94 ± 0.14 with a range of 0.61–1.14. The implication from this observation is that pairs of fibers belonging to the same SR group converge onto the somata of spherical bushy cells by way of their endbulbs.

The form factor value of endbulb 1 is correlated with that of endbulb 2 ($r = 0.707$, $p < 0.01$). These data also address the issue of whether or not fibers of a particular SR group preferentially converge or do not converge upon the same spherical bushy cell (Fig. 5). In this 2 × 2 matrix, the distribution of data points is assumed to indicate the nature of endbulb convergence. If exclusively low SR fibers con-

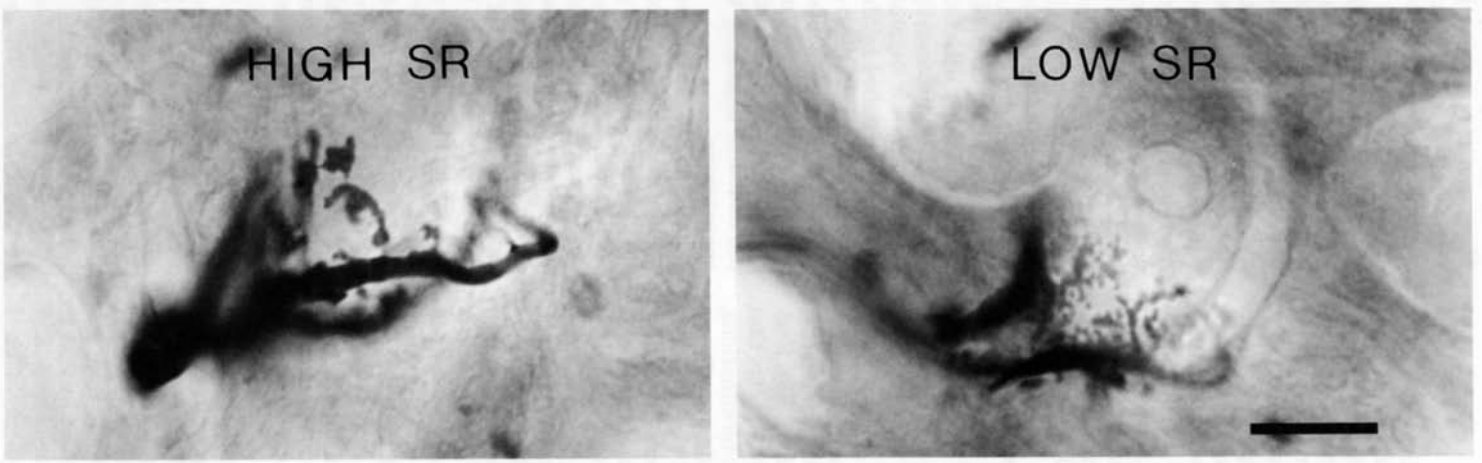

Fig. 1. Photomicrograph of endbulbs from auditory nerve fibers of the different SR groups. The endbulb on the left is from a high SR fiber (CF = 1.1 kHz, SR = 56 s/s); the endbulb on the right is from a low SR fiber (CF = 1.0 kHz, SR = 0.01 s/s). These endbulbs are from the same cat but opposite cochlear nuclei. Note that the endbulb from the low SR fiber has more but smaller lobulations and swellings compared to that of the endbulb from the high SR fiber. SR, spontaneous discharge rate; CF, characteristic frequency. Scale bar equals 10 μm.

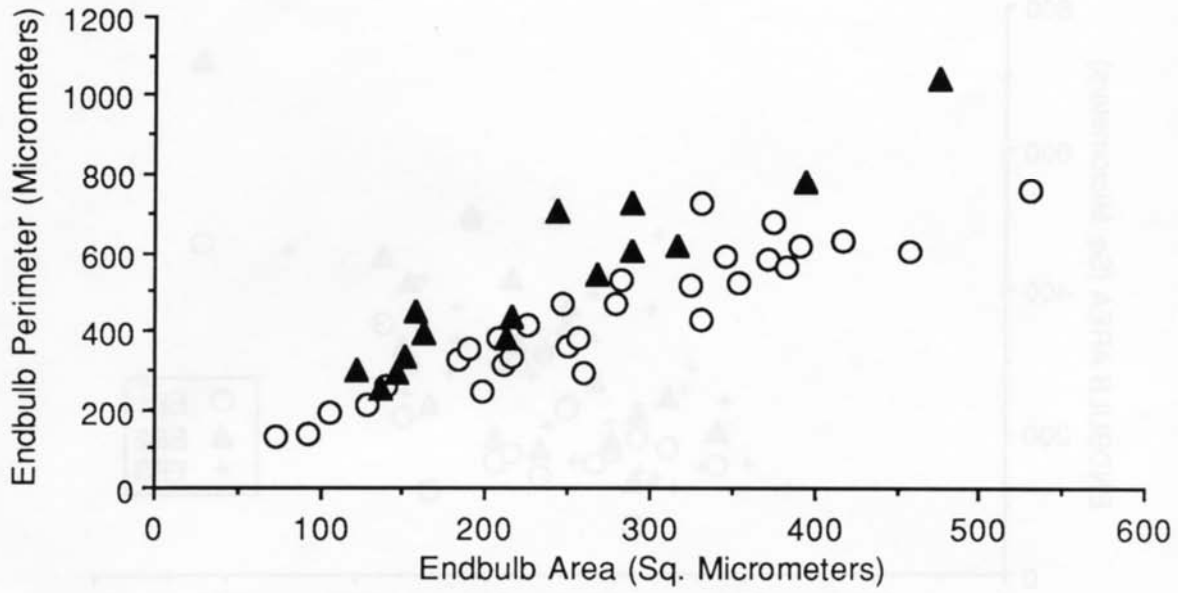

Fig. 2. Scatter plot illustrating the relationship between endbulb area and endbulb perimeter, comparing data from high SR fibers (open circles) and low SR fibers (filled triangles). Although endbulbs of both SR groups overlap in area, endbulbs of low SR fibers tend to have larger perimeters. These data are from endbulbs of 45 fibers which were physiologically characterized and labeled using intracellular techniques.

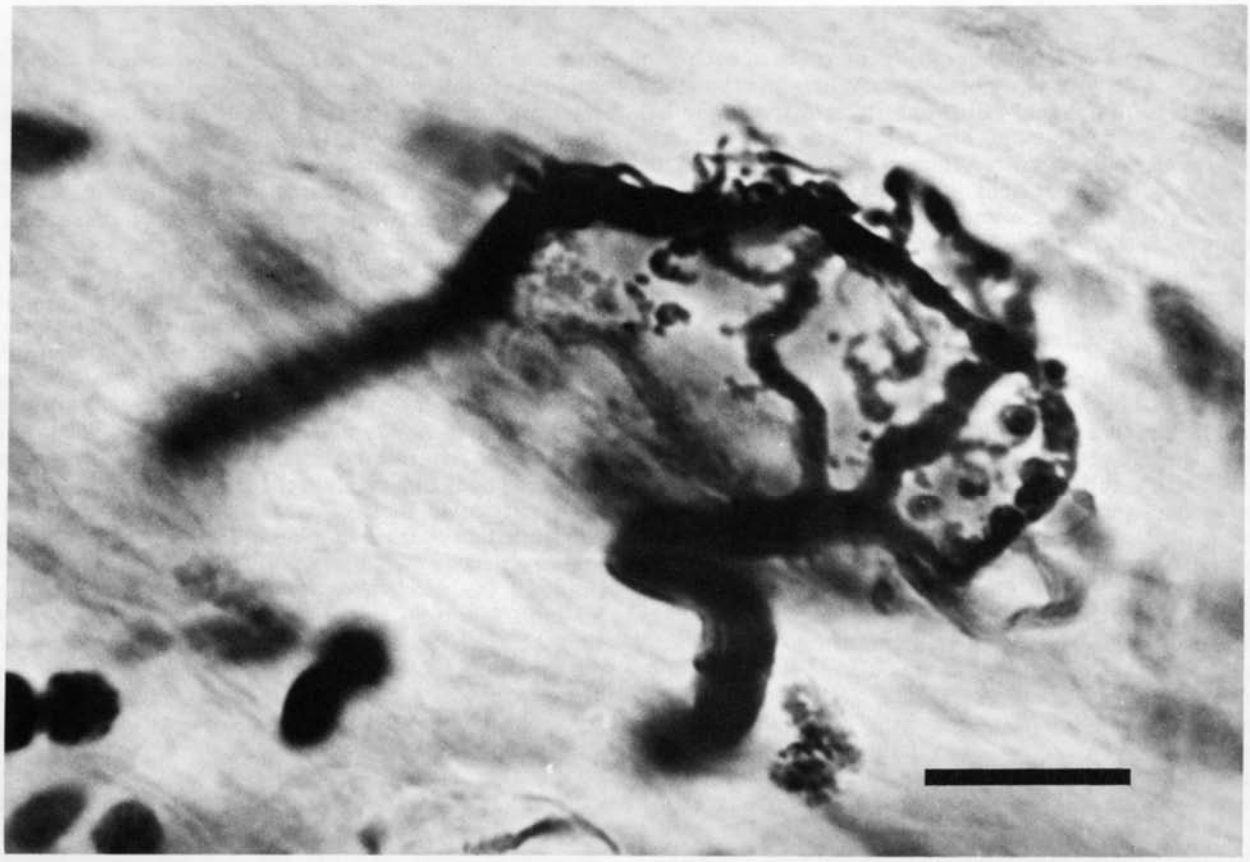

Fig. 3. Photomicrograph of a pair of endbulbs converging upon the same spherical bushy cell in the anterior part of the anteroventral cochlear nucleus. Their coarse appearance and form factors (0.583 and 0.550) are typical for high SR endbulbs. Scale bar equals 10 μm.

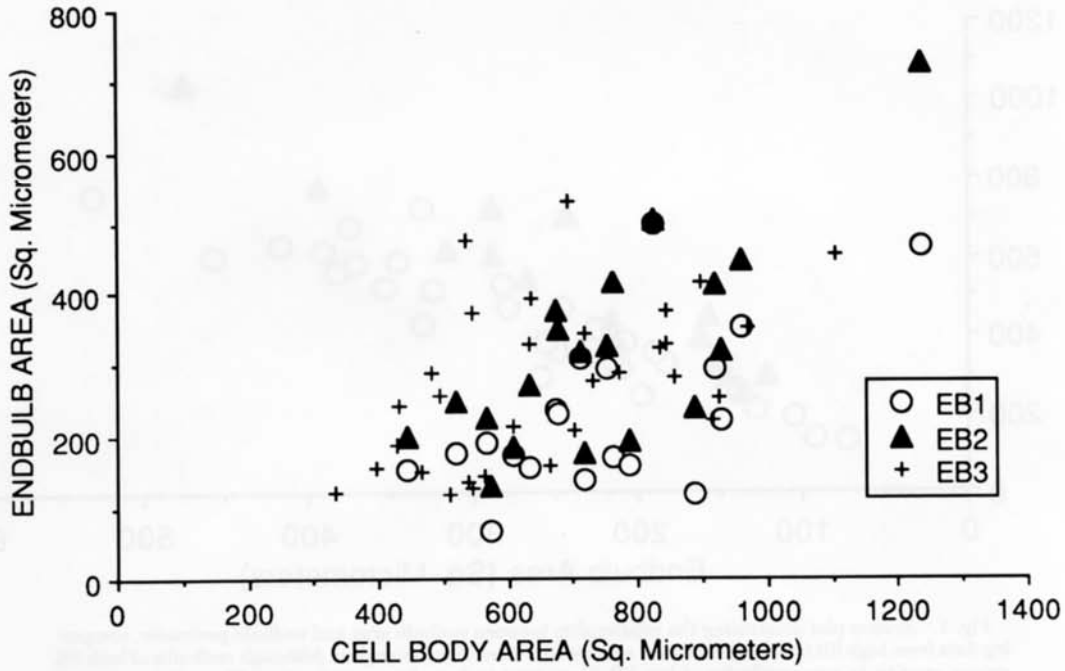

Fig. 4. Scatter plot of endbulb silhouette area (ordinate) versus the area of its postsynaptic cell body (abcissa). The data include endbulb pairs (n = 19), with open circles representing the smaller endbulb (EB1) and solid triangles representing the larger (EB2), plus 31 endbulbs from intracellular labeling experiments (EB3). In general, the larger the cell body, the larger the endbulbs that it receives.

verge by way of endbulb pairs, then members of each pair would be expected to have form factor values less than 0.52 and data points should fall primarily into the lower left quadrant. In contrast, if high SR fibers tend to form convergent endbulb pairs, then data points should lie primarily in the upper right quadrant. Last, if high and low SR fibers tend to form endbulb pairs, then data points should lie in the upper left and lower right quadrants. Our data, albeit limited for endbulb pairs of low SR fibers, imply that convergence occurs in both SR groups.

Electron microscopy

Since our light microscopic data suggest that endbulbs of fibers from different SR groups do not converge, we sought other means that might allow endbulbs of high SR fibers to disperse their activity to additional spherical bushy cells within the anterior division of the AVCN. Our approach was to use electron microscopy to explore the possibility of new synaptic relationships. We selected an HRP-labeled endbulb from an intracellularly labeled and physiologically characterized high SR fiber (CF = 1.4 kHz; SR = 55 s/s). The labeled endbulb arborized around roughly half of the cell body (Fig. 6A), exhibited a silhouette area of 329.9 μm^2, had a form factor of 0.59, and was located in the anterior division of the AVCN (Fig. 6B). The HRP-labeled endbulb converged upon the cell body with a second unlabeled endbulb. Each endbulb arose from the unmyelinated terminal portion of a thick (2.5 μm in diameter), myelinated axon. The endbulb itself consisted of an elaborate network of branches, lobules, and swellings, linked together by thin and unmyelinated processes and extended over the surface of the cell body. Electron microscopy confirmed the labyrinthine appearance of the endbulb as seen with the light microscope. This spherical bushy cell also received two bouton endings each of which arose from separate small diameter (1.1 μm), lightly myelinated axons. We have been unable to follow any of these unlabeled axons sufficiently to determine whether they are connected to the same parent fiber or whether they each arise from separate fibers.

Endbulbs and bouton endings all exhibited internal features that identified them as primary terminals, distinguishable with or without the presence of HRP reaction product (e.g., Cant and Morest, '79b; Ryugo and Fekete, '82; Tolbert and Morest, '82). That is, they contained the usual complement of organelles (mitochondria, microtubules, neurofilaments) plus many clear, large (50–60 nm in diameter), round vesicles. Multiple punctate synaptic contacts were characterized by membrane densities coupled with an accumulation of synaptic vesicles on the presynaptic side of the membrane, and dense, fuzzy material was found in the intercellular cleft. The postsynaptic membrane of the cell body frequently arched toward the endbulb.

Of particular interest was the frequent presence of axodendritic synapses in addition to the numerous axosomatic synapses (see Fig. 7A,B). The postsynaptic membrane of the dendrite typically did not arch toward the endbulb. Montages were not constructed for every section so we can report how many postsynaptic densities were observed but not how many synapses. That is, any single synapse may be represented by postsynaptic densities distributed across 3–7 consecutive sections and we did not determine whether individual postsynaptic densities in adjacent or nearby sections were part of the same or different synapses. Forty-six of 65 montages out of a series of 184 serial sections were quantitatively analyzed; these sections spanned 13.8 μm through the bushy cell body contacted by the labeled endbulb. The top third of the cell and associated endings were not analyzed due to loss of tissue. Primary endings gave rise to 1,340 axosomatic postsynaptic densities and 186 axodendritic postsynaptic

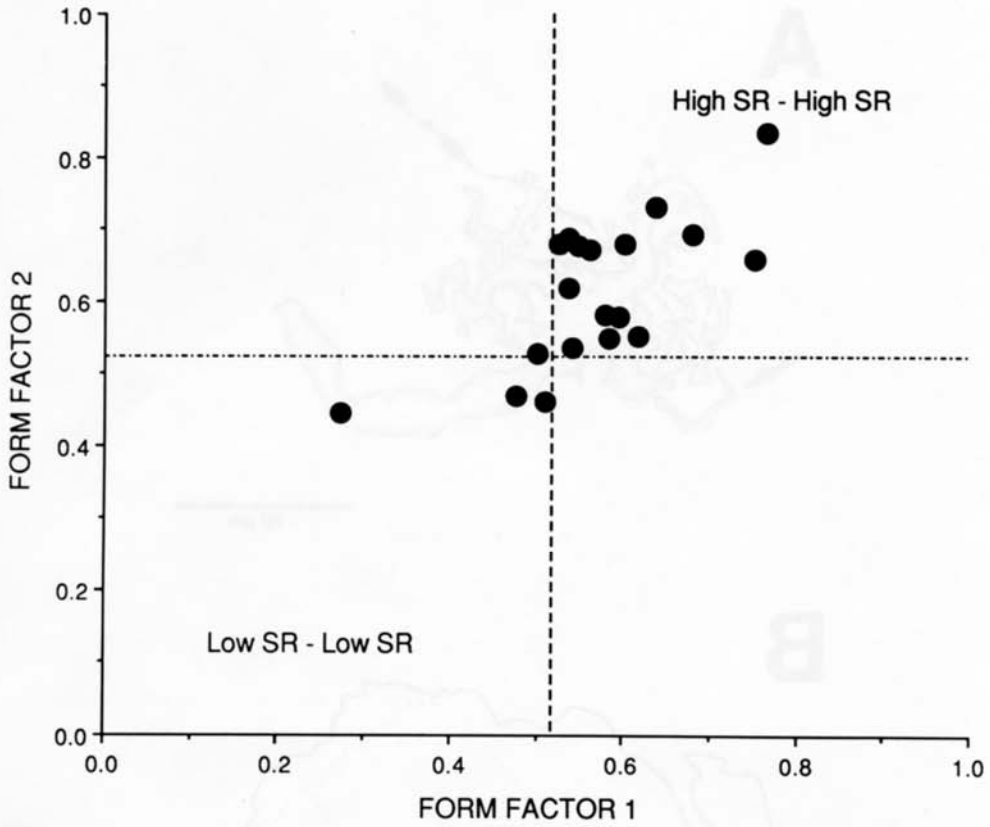

Fig. 5. Scatter plot of the form factor value for the smaller endbulb (abcissa, endbulb 1) versus the form factor value for the larger endbulb (ordinate, endbulb 2) of a pair. Dashed lines are placed at 0.52, which separate form factors of high and low SR fibers (Sento and Ryugo, '89). The data suggest that fibers of both SR groups converge because of the presence of data points in the upper right (High SR–High SR) and the lower left quadrants (Low SR–Low SR). The general lack of data points in the other quadrants suggests that endbulbs from fibers of different SR groups do not mix with one another.

densities. The HRP-labeled endbulb gave rise to 424 axosomatic densities and 50 axodendritic densities; the unlabeled endbulb exhibited 884 axosomatic densities and 118 axodendritic densities. The numerical difference between endbulbs is most likely due to tissue loss that affected analysis of the labeled endbulb more than that of the unlabeled one. The two bouton endings gave rise to 32 axosomatic densities and 18 axodendritic densities. Axodendritic contacts represent 12.8% of the total number of contacts made by the two endbulbs contacting this bushy cell: 11.7% by the labeled endbulb and 13.3% by the unlabeled endbulb. Although the sample is small, 36% of the total number of contacts made by the bouton endings were axodendritic.

In agreement with our light microscopic observations (using Nomarski optics), electron microscopic examination confirmed that the bushy cell had two primary dendrites. One dendrite emerged just above the somatic equator and the other dendrite emerged from the bottom of the cell body. The axon emerged roughly halfway between these dendrites. The labeled endbulb gave rise to a collateral (Fig. 6A, in black), which was myelinated (Fig. 7A) and traveled approximately 65 μm away from the endbulb. A possible target of the collateral is the dendrite, which emerged from the bottom of the cell body contacted by the labeled endbulb.

The presence of axodendritic and axosomatic synapses formed by the same terminal was a regular feature in the 2 cats we examined (Fig. 8). Unlabeled terminals having the cytological features of primary endings (i.e., clear, large round synaptic vesicles and punctate asymmetric membrane densities) had associations with postsynaptic densities of spherical bushy cell somata and with profiles having the appearance of dendrites. Of these unlabeled primary terminals, the larger terminal profiles indicative of endbulbs were more often associated with both axosomatic and axodendritic postsynaptic densities than were the smaller profiles.

Golgi observations

The origin of the dendritic profiles receiving these axodendritic synapses from the endbulbs remains to be definitively determined. Light microscopic examination of Golgi-impregnated cells in the anterior division of the AVCN has provided some relevant clues. Frequently, unstained spheroidal somata containing a round and centrally placed nucleus were visible within the tangle of Golgi-impregnated dendrites of spherical bushy cells (Fig. 9). These unstained somata are inferred to be those of spherical bushy cells on the basis of somatic and nuclear criteria and because the region examined is fairly homogeneous in its neuronal content of spherical bushy cells (Osen, '69; Cant and Morest, '79a). This juxtaposition of cell bodies and dendrites may account for the synaptic relationship between endbulbs, somata of spherical bushy cells, and dendrites of nearby spherical bushy cells.

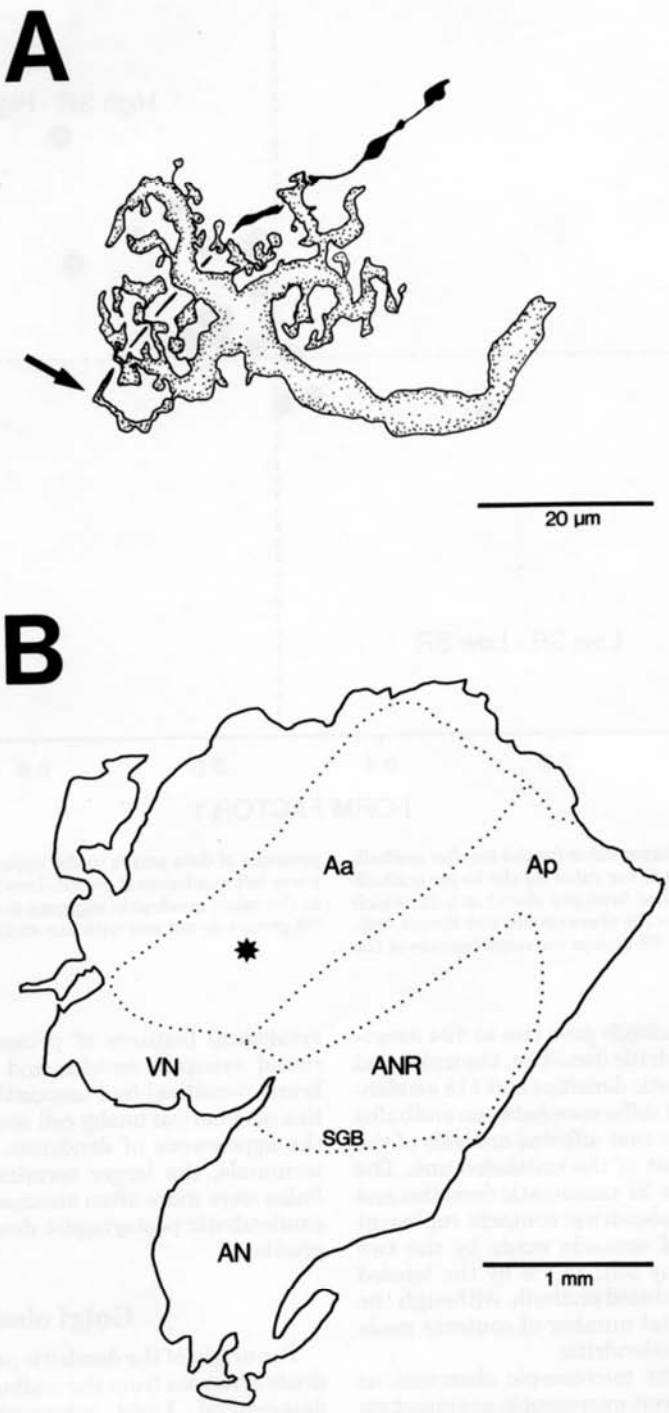

Fig. 6. Endbulb and its location used for electron microscopic study (fiber CF = 1.4 kHz, SR = 55 s/s). **A.** Drawing tube reconstruction of endbulb (stipple). A collateral (in black and indicated by the arrow) extends approximately 65 μm from where it emerges on the endbulb. **B.** Location of this endbulb within the anterior part of the AVCN (asterisk). The plane of section is roughly parallel to the dorsolateral surface of the nucleus. Anterior is to the left and dorsomedial is toward the top. Abbreviations: Aa, anterior division of AVCN; AP, posterior division of AVCN; AN, auditory nerve; ANR, auditory nerve root and region of bifurcations; SGB, Schwann-glia border; VN, vestibular nerve root.

DISCUSSION

In the present study, we applied HRP labeling techniques combined with light and electron microscopy to study the synaptic relationship between endbulbs of Held and spherical bushy cells. Endbulbs have traditionally been described as the large axosomatic endings that arise from the population of thick auditory nerve fibers and terminate in the anteroventral cochlear nucleus (Held, 1893; Ramón y Cajal,

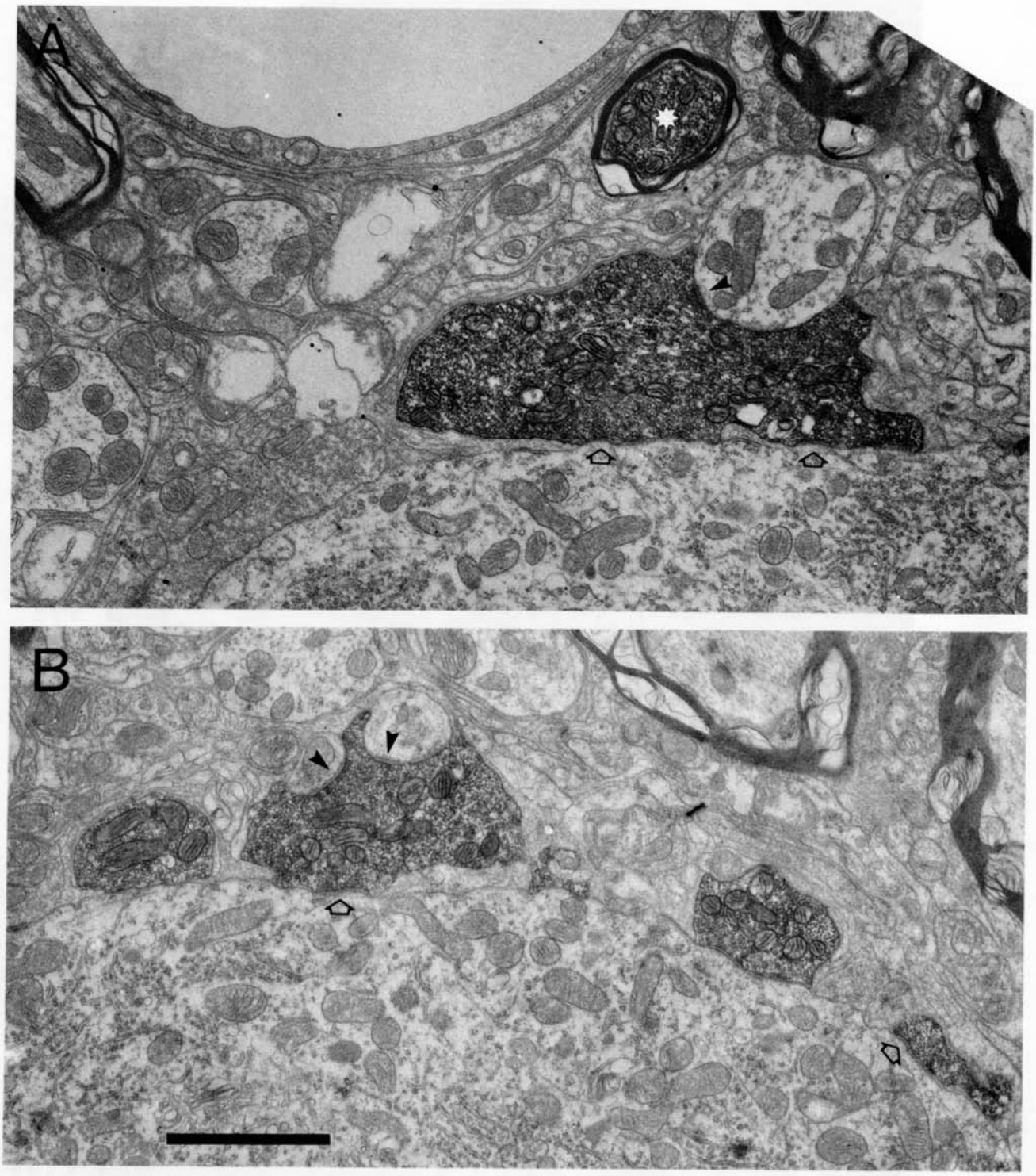

Fig. 7. Electronmicrographs through different regions of the HRP-labeled ending. **A.** View of the endbulb near the emergence of the myelinated collateral (star). This portion of the endbulb makes synaptic contacts with the cell body of the spherical bushy cell (open arrows) and an adjacent dendrite (arrowhead). **B.** Approximately 5 μm away, the labeled endbulb continues to form synapses with the cell body (open arrows) and adjacent dendrites (arrowheads). Axodendritic synapses represented 12% of the contacts made by this endbulb. Scale bar equals 2 μm.

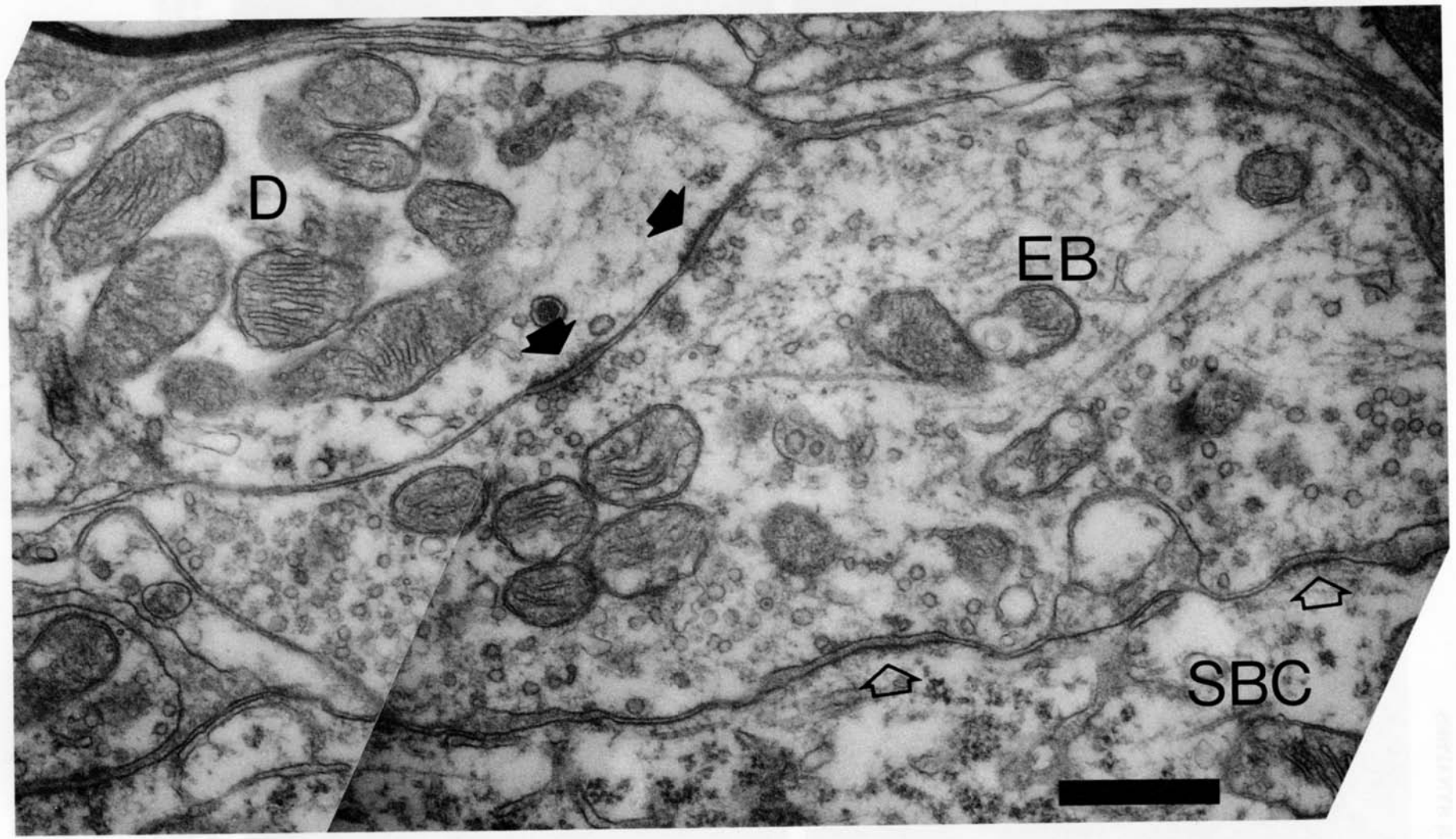

Fig. 8. Electronmicrograph of an unlabeled endbulb (EB) making axodendritic synapses (filled arrows) with a dendrite (D) and axosomatic synapses (open arrows) with a spherical bushy cell (SBC). This spherical bushy cell is within 200 μm of that shown in Figure 7. The cell bodies of spherical bushy cells are ringed by 15–30 dendritic profiles lying within 5 μm of the cell body, many of which receive synapses from primary endings. Scale bar equals 0.5 μm.

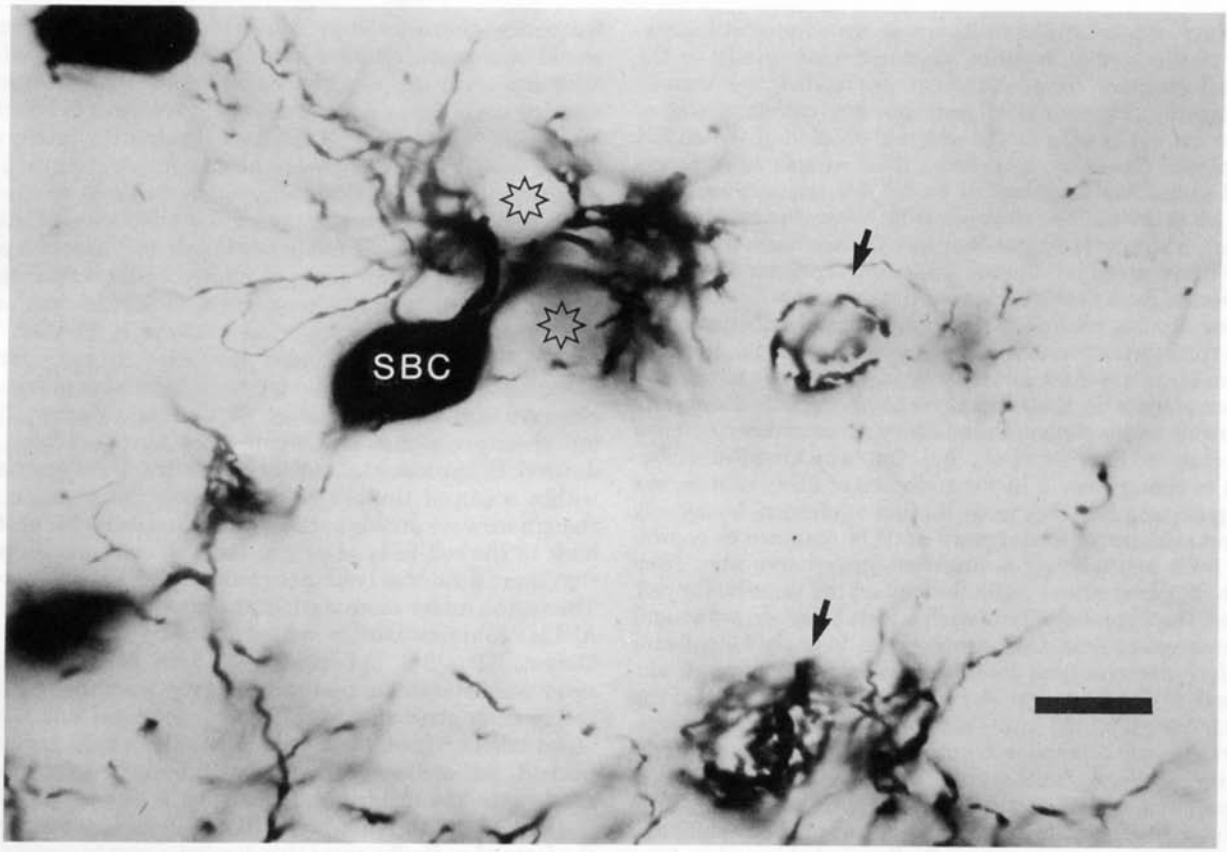

Fig. 9. Photomicrograph of a Golgi-impregnated spherical bushy cell (SBC) in the anterior division of the AVCN. Note that dendrites do not drape back onto their cell body of origin. Furthermore, "hollows" (stars) exist within the dendritic arborization where the somata of presumed spherical bushy cells are found. We hypothesize that these morphological features account for the synaptic relationship between the somata of spherical bushy cells, endbulbs of Held, and dendritic profiles as seen with the electron microscope. Arrows indicate the presence of impregnated endbulbs. Golgi-Kopsch preparation. Scale bar equals 20 μm.

'09; Lorente de Nó, '81). These thick fibers are myelinated (Arnesen and Osen, '78; Cant and Morest, '79b), they arise from type I spiral ganglion neurons whose peripheral processes innervate one, or in rare instances two inner hair cells (Kiang et al., '82; Liberman and Oliver, '84), and the endbulbs terminate exclusively on a distinct class of neurons called spherical bushy cells (Osen, '69; Brawer and Morest, '75; Cant and Morest, '79b; Ryugo and Fekete, '82; Fekete et al., '84; Sento and Ryugo, '89). If from 1–3 endbulbs contact a single neuron (Ramón y Cajal, '09; Lorente de Nó, '81), then one inner hair cell must exert a rapid and powerful influence on a single spherical bushy cell. Our observations confirm and extend current knowledge of endbulb morphology and continue to build the foundation upon which to consider mechanisms of signal processing in the cochlear nucleus.

The endbulb of Held, containing numerous synaptic active zones and having an extensive apposition with the postsynaptic cell body, is presumed to transfer faithfully spike activity in the auditory nerve fiber to the postsynaptic spherical bushy cell. In addition, the endbulb may account for the presence of a small positive prepotential associated with units having primarylike discharge patterns (Pfeiffer, '66; Bourk, '76). This prepotential, although variable in size and shape, is thought to reflect a depolarization in the endbulb and precedes the discharge in the postsynaptic primarylike unit by 0.5 msec (Molnar and Pfeiffer, '68). This 0.5-msec interval is attributed to the synaptic delay. In this context, spherical bushy cells should preserve the signals from the nerve, and the population of primarylike units with prepotentials should reflect the physiological characteristics of the population of auditory nerve fibers. Although spherical bushy cells preserve the temporal patterns of spike discharges as evident in poststimulus time histograms (Rhode et al., '83), they do not appear to preserve SR (Molnar and Pfeiffer, '68). In the auditory nerve, approximately 40% of the fibers have SR $\leq$ 20 s/s and the rest have SR $>$ 20 s/s (Kiang et al., '65; Liberman, '78; Evans and Palmer, '80). Extracellular recordings in the AVCN, however, reveal that less than 15% of primarylike units with an unambiguous prepotential have SR $<$ 20 s/s (Molnar and Pfeiffer, '68). This comparison of data from the nerve and nucleus might be subject to some concern because of possible distortions resulting from incomplete sampling. In addition, the variability of the prepotential might cause some primarylike units with prepotentials to be overlooked. Both circumstances could artificially lower the incidence of low SR primarylike units with prepotentials.

The above concerns are mitigated, however, by data from Yin and his collaborators (unpublished results). These investigators are staining axons of the trapezoid body in cats after first intra-axonally recording their physiological response properties. Of particular interest is the histologic

recovery of primarylike units whose axons project bilaterally to the medial superior olive and ipsilaterally to the lateral superior olive. Although cell bodies are usually unstained, the axonal trajectories are characteristic of spherical bushy cells in the anterior division of the AVCN (Cant and Casseday, '86). From their sample of 19 recovered axons having spherical bushy cell trajectories, none had SR < 20 s/s. The evidence from these separate lines of research clearly indicates that the SR distribution in auditory nerve fibers is different from that of primarylike units (spherical bushy cells) in the cochlear nucleus.

Our studies explore possible anatomical substrates for this transformation of SR from nerve to nucleus. Auditory nerve fibers are most certainly involved because all spontaneous activity in the ventral cochlear nucleus disappears following transection of the auditory nerve or destruction of the cochlea (Koerber et al., '66). One way for SR distribution to change would be for endbulbs of fibers of different SR groups to converge upon the same spherical bushy cell. Direct evidence of convergence could be obtained by recording from and labeling a single auditory nerve fiber from each SR group whose endbulbs contact the same bushy cell. Given the improbability of such a feat, however, we sought an indirect answer. Our strategy was to apply form factor analysis to convergent endbulb pairs with unknown physiological features. Pairs of endbulbs having similar form factor values would imply convergence within SR groups; pairs having dissimilar form factor values would imply convergence across SR groups. The results summarized in Figure 5 demonstrate that endbulb pairs converging onto the same cell body have very similar form factor values and suggest that convergent endbulbs probably arise from fibers of the same SR group.

SR proportions in the cochlear nucleus could also be transformed if high SR auditory nerve fibers gave rise to more endbulbs than did low SR fibers. This situation, however, is not the case because individual auditory nerve fibers give rise to the same average number of endbulbs (Ryugo and Rouiller, '88). Furthermore, if endbulbs of low SR fibers converge but endbulbs of high SR fibers do not, SR distribution could be increased in the nucleus. Form factor analysis (e.g., Fig. 5) indicates that fibers of both SR groups converge.

There remains unsolved issues that might yet account for the transformation of SR from nerve to nucleus. For example, the convergence of 2 low SR fibers could convert the postsynaptic cell to a high SR primarylike unit. The paucity of auditory nerve fibers having SR between 10–40 s/s (see Fig. 9 of Liberman, '78) diminishes such a possibility. In other words, the summed discharges of a pair of low SR fibers would rarely exceed 20 s/s, so SR grouping would not change for the primarylike unit. It also remains to be determined whether collaterals arising from the endbulb (Brawer and Morest, '75; Lorente de Nó, '81; Ryugo and Fekete, '82; Sento and Ryugo, '89) disperse sufficient activity for altering the proportion of SR from nerve to nucleus.

Incidently, it is difficult to account for the relatively infrequent observations of HRP-labeled convergent endbulbs at the light microscopic level. One possibility is that convergent endbulbs arise from fibers innervating separate loci (and thus, separate frequency domains) of the cochlea. We dismiss this notion because the sharpness of tuning (Q_{10} value) of prepotential units is indistinguishable from that of auditory nerve units (Bourk, '76); if fibers of different frequency characteristics converged, prepotential units would be expected to have broader frequency sensitivities. Evidence from our electron microscopic studies suggests that spherical bushy cells tend to receive pairs of endbulbs. The light microscopic HRP data apparently produce a biased view of how many endbulbs actually converge. This situation could result since convergent axons do not necessarily travel together and extracellular injections of HRP in the nerve might simply fail to label both members of a pair.

With the aid of the electron microscope, we discovered that endbulbs, typically considered to furnish powerful axosomatic synapses to spherical bushy cells (Pfeiffer, '66; Kiang, '75; Bourk, '76), also gave rise to axodendritic synapses. Such axodendritic synapses have been previously observed (e.g., Lenn and Reese, '66; Cant and Morest, '79b), but their prevalence and significance have not been addressed. In our material, the target dendrites were all found within 5 μm of the cell body receiving the endbulb. Although we were unable to trace individual dendritic profiles back to the cell body of origin, indirect evidence suggests that these dendrites belong to nearby spherical bushy cells. The region under examination (the anterior division of the AVCN) contains mostly spherical bushy cells (Cant and Morest, '79a, '84). Spherical bushy cells emit several primary dendritic stalks that radiate away from the cell body before each gives rise to a "bushy" terminal tuft. These distal arbors do not "feed back" upon the parent cell body; instead, cell bodies of other spherical bushy cells tend to nestle into the dendritic arbors (Fig. 9; see also Figures 3–12 and 3–15 in Lorente de Nó, '81). Primary endings in the form of endbulbs enter this dendritic nest to contact the dendrites and the cell body they harbor (Fig. 10). The labeled high SR endbulb and the unlabeled (but presumably high SR) endbulb each formed 12% of their synapses against neighboring dendrites. It is unknown how these dendritic synapses might affect SR because we do not know precisely how many synapses are formed, the strength of synaptic drive, how distant these synapses are from the spike generator, how many dendrites from different spherical bushy cells are involved, or what the target neuron's membrane characteristics are. Nevertheless, it appears that these axodendritic synapses from endbulbs of high SR fibers represent one mechanism by which auditory nerve fiber activity is dispersed to multiple spherical bushy cells and how the proportion of low SR in the nerve is reduced in the nucleus.

A final comment about the morphological similarity among endbulb pairs that arise from separate neurons: The form factor for individual endbulbs yields an objective parameter that accurately corresponded to the parent fiber's SR. There was a broad range of form factor values for individual endbulbs, but pairs of endbulbs exhibited nearly identical form factor values. In fact, the variability of form factor values among endbulb pairs is much less than that among the subpopulation of high or low SR auditory nerve fibers. These observations add to the concept that axons of different origins can form morphologically similar terminations on the same target, as in the case of mossy fiber endings (Palay and Chan-Palay, '74). In the context that individual auditory nerve fibers form morphologically distinct endings on different target neurons in the cochlear nucleus (e.g., Lorente de Nó, '33; Rouiller et al., '86), we lend support to the argument that the postsynaptic target

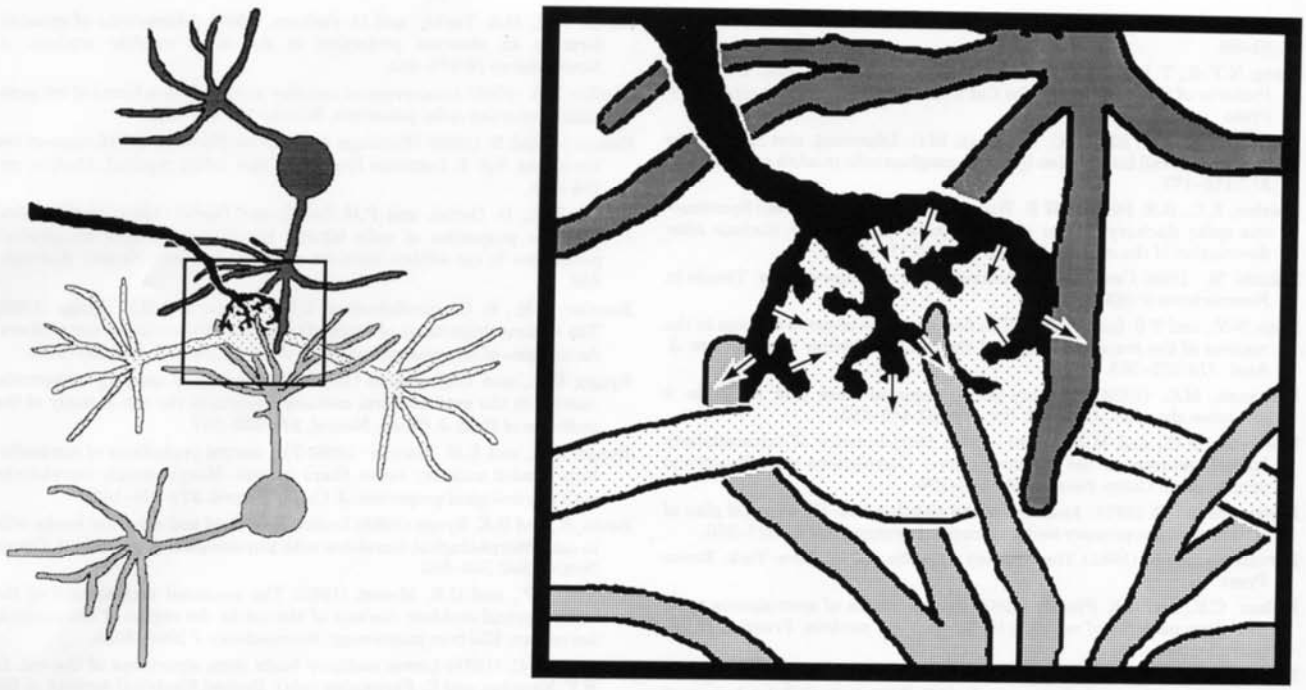

Fig. 10. Schematic diagram of hypothesized synaptic relationships between a single endbulb, the cell body of its postsynaptic spherical bushy cell, and the dendrites of adjacent spherical bushy cells. Arrows indicate the direction of flow for synaptic information.

influences the form of the presynaptic terminal (Mugnaini, '71; Campbell and Frost, '88; Parks et al., '90).

This line of thought leads to another question: How does the synaptic relationship between converging endbulbs and spherical bushy cells develop? If a fiber's SR is determined quite early, for example, by its peripheral morphology and connections with the inner hair cell, then two endbulbs from separate neurons but of the same SR group must find the same spherical bushy cell upon which to converge. Such a situation would require rather specific signaling during axonal outgrowth and synaptogenesis. Alternatively, undifferentiated endbulbs could converge without SR restrictions, and the spherical bushy cell could subsequently influence the physiology and morphology of the afferent neurons. Although it remains to be determined how these connections are formed, the pre- and postsynaptic components are sufficiently identifiable that experiments using this system might help resolve the issue.

ACKNOWLEDGMENTS

This work was supported by NIH grant R01 DC00232. The authors thank Tan Pongstaporn for his technical assistance with electron microscopy, and Bradford J. May, George A. Spirou, and Debora D. Wright for helpful discussions and comments on the manuscript. We also thank Dr. Tom C.T. Yin of the University of Wisconsin for sharing his unpublished data with us.

LITERATURE CITED

Adams, J.C. (1979) A fast, reliable silver-chromate Golgi method for perfusion-fixed tissue. Stain Technol. *54:*225–226.

Arnesen, A.R., and K.K. Osen (1978) The cochlear nerve in the cat: Topography, cochleotopy, and fiber spectrum. J. Comp. Neurol. *178:*661–678.

Bourk, T.R. (1976) Electrical Responses of Neural Units in the Anteroventral Cochlear Nucleus of the Cat. Ph.D. dissertation, Massachusetts Institute of Technology.

Brawer, J.R., and D.K. Morest (1975) Relations between auditory nerve endings and cell types in the cat's anteroventral cochlear nucleus seen with the Golgi method and Nomarski optics. J. Comp. Neurol. *160:*491–506.

Campbell, G., and D.O. Frost (1988) Synaptic organization of anomalous retinal projections to the somatosensory and auditory thalamus: Target-controlled morphogenesis of axon terminals and synaptic glomeruli. J. Comp. Neurol. *272:*383–408.

Cant, N.B., and J.H. Casseday (1986) Projections from the anteroventral cochlear nucleus to the lateral and medial superior olivary nuclei. J. Comp. Neurol. *247:*457–476.

Cant, N.B., and D.K. Morest (1979a) Organization of the neurons in the anterior division of the anteroventral cochlear nucleus of the cat. Light microscopic observations. Neuroscience *4:*1909–1923.

Cant, N.B., and D.K. Morest (1979b) Bushy cells in the anteroventral cochlear nucleus of the cat. A study with the electron microscope. Neuroscience *4:*1925–1945.

Cant, N.B., and D.K. Morest (1984) The structural basis for stimulus coding in the cochlear nucleus of the cat. In C.I. Berlin (ed): Hearing Science: Recent Advances. San Diego: College-Hill Press, pp. 371–421.

Colonnier, M. (1964) The tangential organization of the visual cortex. J. Anat. *98:*327–344.

Evans, E.F., and A.R. Palmer (1980) Relationship between the dynamic range of cochlear nerve fibers and their spontaneous activity. Exp. Brain Res. *40:*115–118.

Fekete, D.M., E.M. Rouiller, M.C. Liberman, and D.K. Ryugo (1984) The central projections of intracellularly labeled auditory nerve fibers in cats. J. Comp. Neurol. *229:*432–450.

Held, H. (1893) Die centrale Gehörleitung. Arch. Anat. Physiol., Anat. Abt. 201–248.

Ibata, Y., and G.D. Pappas (1976) The fine structure of synapses in relation to the large spherical neurons in the anterior ventral cochlear [sic] of the cat. J. Neurocytol. *5:*395–406.

Kiang, N.Y.S. (1975) Stimulus representation in the discharge pattern of auditory neurons. In D.B. Tower (ed.): The Nervous System, Vol. 3,

Human Communication and its Disorders. New York: Raven Press, pp. 81–96.

Kiang, N.Y.-S., T. Watanabe, E.C. Thomas, and L.F. Clark (1965) Discharge Patterns of Single Fibers in the Cat's Auditory Nerve. Cambridge: MIT Press.

Kiang, N.Y.S., J.M. Rho, C.C. Northrup, M.C. Liberman, and D.K. Ryugo (1982) Hair-cell innervation by spiral ganglion cells in adult cats. Science *217:*175–177.

Koerber, K.C., R.R. Pfeiffer, W.B. Warr, and N.Y.S. Kiang (1966) Spontaneous spike discharges from single units in the cochlear nucleus after destruction of the cochlea. Exp. Neurol. *16:*119–130.

Konishi, M. (1986) Centrally synthesized maps of sensory space. Trends in Neuroscience *9:*163–168.

Lenn, N.Y., and T.S. Reese (1966) The fine structure of nerve endings in the nucleus of the trapezoid body and the ventral cochlear nucleus. Am. J. Anat. *118:*375–389.

Liberman, M.C. (1978) Auditory-nerve response from cats raised in a low-noise chamber. J. Acoust. Soc. Am. *63:*442–455.

Liberman, M.C., and M.E. Oliver (1984) Morphometry of intracellularly labeled neurons of the auditory nerve: Correlations with functional properties. J. Comp. Neurol. *223:*163–176.

Lorente de Nó, R. (1933) Anatomy of the eighth nerve. III. General plan of structure of the primary cochlear nuclei. Laryngoscope *43:*327–350.

Lorente de Nó, R. (1981) The Primary Acoustic Nuclei. New York: Raven Press.

Molnar, C.E., and R.R. Pfeiffer (1968) Interpretation of spontaneous spike discharge patterns of neurons in the cochlear nucleus. Proceed. IEEE, *56:*993–1004.

Mugnaini, E. (1971) Developmental aspects of synaptology with special emphasis on the cerebellar cortex. In D.C. Pease (ed): Cellular Aspects of Neural Growth and Differentiation. Los Angeles: Univ. of Calif. Press, pp. 141–165.

Osen, K.K. (1969) Cytoarchitecture of the cochlear nuclei in the cat. J. Comp. Neurol. *136:*453–484.

Palay, S.L., and V. Chan-Palay (1974) The Cerebellar Cortex, New York: Springer-Verlag.

Parks, T.N., D.A. Taylor, and H. Jackson (1990) Adaptations of synaptic form in an aberrant projection to the avian cochlear nucleus. J. Neuroscience *10:*975–984.

Pfeiffer, R.R. (1966) Anteroventral cochlear nucleus: Wave forms of extracellularly recorded spike potentials. Science *154:*667–668.

Ramón y Cajal, S. (1909) Histologie du Système Nerveux de l'Homme et des Vertébrés, Vol. I. Instituto Ramón y Cajal (1952 reprint), Madrid, pp. 754–838.

Rhode, W.S., D. Oertel, and P.H. Smith and Oertel (1983) Physiological response properties of cells labeled intracellularly with horseradish peroxidase in cat ventral cochlear nucleus. J. Comp. Neurol. *213:*448–463.

Rouiller, E.M., R. Cronin-Schreiber, D.M. Fekete, and D.K. Ryugo (1986) The central projections of intracellularly labeled auditory nerve fibers: An analysis of terminal morphology. J. Comp. Neurol. *249:*261–278.

Ryugo, D.K., and D.M. Fekete (1982) Morphology of primary axosomatic endings in the anteroventral cochlear nucleus of the cat: A study of the endbulbs of Held. J. Comp. Neurol. *210:*239–257.

Ryugo, D.K., and E.M. Rouiller (1988) The central projections of intracellularly labeled auditory nerve fibers in cats: Morphometric correlations with physiological properties. J. Comp. Neurol. *271:*130–142.

Sento, S., and D.K. Ryugo (1989) Endbulbs of Held and spherical bushy cells in cats: Morphological correlates with physiological properties. J. Comp. Neurol. *280:*553–562.

Tolbert, L.P., and D.K. Morest (1982) The neuronal architecture of the anteroventral cochlear nucleus of the cat in the region of the cochlear nerve root: Electron microscopy. Neuroscience *7:*3053–3030.

Tsuchitani, C. (1978) Lower auditory brain stem structures of the cat. In R.F. Naunton and C. Fernandex (eds): Evoked Electrical Activity in the Auditory Nervous System. New York: Academic Press, pp. 373–401.

Van der Loos, H. (1959) Une combinaison de deux vielles methodes histologiques pour le systeme nerveux central. Mschr. Psychiat. Neurol. *132:*330–334.

Warr, W.B. (1982) Parallel ascending pathways from the cochlear nucleus. Contri. Sens. Physiol. *7:*1–38.